Chemical Engineering Journal 485 (2024) 149849

Contents lists available at ScienceDirect

Chemical Engineering Journal

journal homepage: www.elsevier.com/locate/cej

Alginate aerogels by spray gelation for enhanced pulmonary delivery and solubilization of beclomethasone dipropionate

Thoa Duong [a], Maria Vivero-Lopez [a], Inés Ardao [b], Carmen Alvarez-Lorenzo [a], Attila Forgács [c], József Kalmár [c,*], Carlos A. García-González [a,*]

[a] AerogelsLab, I+D Farma Group (GI-1645), Department of Pharmacology, Pharmacy and Pharmaceutical Technology, Faculty of Pharmacy, iMATUS and Health Research Institute of Santiago de Compostela (IDIS), Universidade de Santiago de Compostela, E-15782 Santiago de Compostela, Spain
[b] BioFarma Research Group, Department of Pharmacology, Pharmacy and Pharmaceutical Technology, Innopharma Drug Screening and Pharmacogenomics Platform, Centro Singular de Investigación en Medicina Molecular y Enfermedades Crónicas (CiMUS), Universidade de Santiago de Compostela, E-15782 Santiago de Compostela, Spain
[c] HUN-REN-DE Mechanisms of Complex Homogeneous and Heterogeneous Chemical Reactions Research Group, Department of Inorganic and Analytical Chemistry, University of Debrecen, Egyetem tér 1, Debrecen H-4032, Hungary

ARTICLE INFO

Keywords:
Pulmonary drug delivery
Supercritical fluids
Aerogels
Hydration
Beclomethasone dipropionate

ABSTRACT

Aerogel technology is an emerging platform that offers alternative and cost-effective dry carriers with advanced performances for the pharmaceutical industry. The innovative combination of compressed air-assisted spray gelation and "green" supercritical fluid (SCF) technology was used in this study to produce alginate aerogel microparticles with adequate properties for pulmonary drug delivery. Beclomethasone dipropionate (BDP), a poorly water-soluble anti-inflammatory drug for asthma treatment, was loaded into alginate aerogel particles by SCF-assisted impregnation ensuring high loading, as well as the amorphization of the drug. The production of aerogels was optimized through the fine-tuning of parameters in compressed air-assisted spray gelation, specifically adjusting the air flow rate and the pump speed. Alginate aerogels were aimed to be produced with an appropriate aerodynamic diameter from 1 to 5 μm, measured by *in vitro* deposition tests with Next Generation impactor and potential for deep lung penetration. Nuclear magnetic resonance (NMR) relaxometry was used to assess aerogel hydration and unveiled structure–property relationships leading to the sudden release of the drug. Finally, *in vitro* cytotoxicity tests in fibroblasts and *ex vivo* permeability tests were conducted. These biological tests confirmed the excellent biocompatibility of the aerogel formulations and demonstrated the efficient deposition of BDP in porcine bronchial tissues assisted by the porous alginate aerogel carrier.

1. Introduction

Pulmonary drug delivery is an effective strategy for the local treatment of lung diseases such as asthma, chronic obstructive pulmonary disease (COPD) or cystic fibrosis [1–3]. Pulmonary drug dosage forms allow the delivery of drugs to the site of action, improving the therapeutic outcomes while minimizing systemic side effects [4–6]. Aerogels are gaining increasing attention as pulmonary drug delivery systems because of their extremely low bulk density, which allows producing large porous microparticles with excellent aerodynamic diameters [7,8]. The 3D-structure of an aerogel consists of a highly porous solid network with interconnected mesoporosity, which confers high specific surface area and low bulk density [9–11].

Aerogels made of alginate are biocompatible and biodegradable, and their mucoadhesive properties can be exploited for the delivery of drugs to mucosal tissues at a precisely targeted site [12–14]. Alginate aerogels for pulmonary administration should have suitable aerodynamic size in the 1–5 μm range, low cohesive forces, low bulk density, high homogeneity, and high flowability [7,9,10,15]. Alginate is not a component of commercial dry powder inhaler (DPI) formulations yet, but clinical trials have demonstrated that low molecular-weight alginate is safe and well tolerated in humans after multiple dose inhalation (FDA clinical trial NCT02157922) [16]. Alginate structural features and gelation processing variables affect the stability of alginate aerogels as well as how effectively drugs are released through swelling-dissolution-erosion mechanisms [17]. Alginate hydrogels are typically prepared by ionic

* Corresponding authors.
E-mail addresses: kalmar.jozsef@science.unideb.hu (J. Kalmár), carlos.garcia@usc.es (C.A. García-González).

https://doi.org/10.1016/j.cej.2024.149849
Received 18 November 2023; Received in revised form 27 January 2024; Accepted 18 February 2024
Available online 20 February 2024

gelation of alginate with divalent cations, which can be supplied either externally (by dropping of alginate solution in a gelation bath containing cations), or internally through a pH-driven release of cations making them available to alginate [10,18]. The solvated gels are formulated into aerogels through the extraction of the solvent by supercritical CO_2 ($scCO_2$) [19,20].

A highly reproducible and scalable processing strategy is needed for the preparation of alginate aerogel microparticles of certain shape and size, homogeneous particle size distribution and good flow dispersibility for the respiratory system. Alginate gel particles obtained by conventional prilling methods resulting in spherical particles with sizes of few milimeters were typically not compatible with the intended delivery application [18]. Alternatively, alginate aerogel microspheres with suitable aerodynamic diameters in the 1–5 μm range, and narrow particle size distribution were obtained by inkjet printing technique [9]. Unfortunately, this technique has a limited scalability in terms of throughput. The emulsion-gelation method was also used to prepare inhaled alginate microspheres, but additional steps were needed for oil removal [12].

Compressed air-assisted prilling gelation emerges as an efficient, scalable and simple process for the preparation of alginate aerogels for pulmonary drug delivery. This technique uses compressed air to break fluid streams into droplets through nozzles creating pressure differences [21]. In this work, the combination of compressed air-assisted prilling gelation with supercritical fluid (SCF) technology was developed to produce calcium alginate aerogel microspheres suitable for pulmonary drug delivery.

Different loading strategies have been proposed for the incorporation of bioactive compounds into aerogels: (i) before gelation, (ii) during solvent exchange, (iii) during drying, or (iv) via $scCO_2$ impregnation [11]. The choice mainly depends on the solubility of the drug in water, ethanol and $scCO_2$. Beclomethasone dipropionate (BDP), an anti-inflammatory medication for asthma patients, is extremely insoluble in aqueous solvents, therefore, it is not a feasible candidate for loading into aerogels using strategies (i) to (iii). BDP can be incorporated into aerogels by $scCO_2$ impregnation due to the high density of $scCO_2$ (0.2–1.5 g/cm^3) and its ability to penetrate polymer matrices in mild conditions [22].

In this work, aerogel carriers were prepared by compressed air-assisted prilling gelation followed by $scCO_2$ drying. The particle size distribution of gels obtained by the compressed air-assisted prilling gelation method was studied as a function of air and liquid stream flows. Morphological and textural properties of the alginate aerogels were assessed through SEM imaging and nitrogen adsorption–desorption analysis. BDP was impregnated into these alginate aerogel particles under $scCO_2$-assisted conditions. The effect of impregnation time (1–9 h) on the resulting BDP-loaded alginate aerogel regarding the matrix structure, hydration properties (erosion and swelling), drug-carrier interactions and BDP release profiles was evaluated. The aerodynamic properties of the loaded aerogel powders were determined using a Next Generation Impactor (NGI). X-ray diffraction, ATR and DSC were conducted to evaluate the solid state structure and the intermolecular forces between the drug and the carrier. Nuclear magnetic resonance (NMR) relaxometry was employed to predict aerogel particle behavior in aqueous environments. *In vitro* cytotoxicity tests in fibroblasts were employed to assess the potential toxic effects of inhaled formulation. Finally, *ex vivo* permeability tests were conducted on porcine bronchial tissue to evaluate the ability of the inhaled formulation to penetrate and be absorbed in the bronchial tissue.

2. Materials and methods

2.1. Materials

Beclomethasone dipropionate (BDP, Mw = 521.05 g/mol, white powder, purity >98 %) was obtained from Tokyo Chemical Industry Co., Ltd (Tokyo, Japan). Alginic acid sodium salt extracted from brown algae (guluronic acid/mannuronic acid ratio of 70/30, Mw = 403 kDa) was provided by Sigma Aldrich (Irvine, UK). Calcium chloride ($CaCl_2$) was supplied from Merck (Darmstadt, Germany). Carbon dioxide (CO_2 > 99.8 % purity) was purchased from Nippon Gases (Madrid, Spain). Acetone (100 % purity) was provided from Scharlau Chemie S.A (Barcelona, Spain) and absolute ethanol from Merck (Darmstadt, Germany).

2.2. Determination of operating window for alginate aerogel production

Calcium alginate aerogel powder was prepared by a prilling gelation method using a compressed air-assisted spraying equipment (Surplus Solutions LLC, Woonsocket, RI, USA) (Fig. 1), followed by solvent exchange with ethanol and the subsequent drying via a continuous flow of $scCO_2$.

An aqueous sodium alginate solution of 1.75 % (w/v) was prepared by mechanical stirring (500 rpm) at room temperature for 4 h. Afterwards, the alginate solution (20 mL) was transferred using a silicone tube to a nozzle for spraying into 200 mL of an aqueous 150 mM $CaCl_2$ solution. A variety of spraying conditions were examined, as listed in Table 1. The pump speed (300 and 750 rpm) and the air flow rate (30–50 L/min, responsible for pulverizing the solution) were varied to determine the optimal conditions for the production of alginate aerogel microspheres. The diameter of the nozzle (0.4 mm), the height from the nozzle to the bath of $CaCl_2$ (25 cm) and the stirring rate (500 rpm) were maintained constant. Ageing of alginate hydrogels took place for 2 h in the $CaCl_2$ solution before solvent exchange with ethanol. The hydrogels were directly placed in absolute ethanol, which was changed three times in every 24 h. Alginate alcogels were dried using $scCO_2$ (40 °C, 120 bar) at a flow of 5 g/min during 3.5 h in an autoclave (Thar Technologies, Pittsburgh, PA, USA). Afterwards, the diameter of the collected aerogel particles was determined by SEM imaging and digital data analysis with ImageJ bundled with 64-bit Java 8 software (National Institutes of Health, NIH, USA). When the particle sizes follow a normal distribution or log-normal distribution, the frequency histogram displays a symmetrical, Gaussian bell shape, with a vertical symmetrical axis passing through the maximum point [23]. In this study, the log-normal distribution (with higher R^2 value) (Fig. S1), was employed for plotting alongside the probit number (P) and in calculating the average particle size.

The calculation for the obtained size distribution of each formulation is showed in Table 1 and in Fig. S1, and explained in the Supporting Information.

2.3. Preparation of BDP-loaded alginate aerogels

The as-prepared alginate aerogel microspheres were loaded with BDP. Alginate aerogel (0.40 g) and BDP (0.040 g) powders were poured in separate paper cartridges (Filter paper reams, 75 g/m^2, Scharlab, Barcelona, Spain) and placed within the 100-mL autoclave of the equipment, which was previously loaded with 5 mL (5 % vol.) acetone. $ScCO_2$ impregnation was conducted at 65 °C and 215 bar using different contact times (1, 2, 6, and 9 h). Afterwards, the depressurization rate was set at 1 g/min until reaching atmospheric pressure. Fixed conditions were pressure (215 bar), temperature (65 °C), and weight ratio (1:10) of BDP and alginate aerogel.

2.4. BDP loading yield

The BDP-loaded alginate aerogels were immersed into acetonitrile/water (ACN:H_2O, 65:35 % v/v), followed by sonication to release all BDP from the formulation. BDP content was quantitatively determined using a JASCO HPLC (Tokyo, Japan) (AS-4150 Autosampler, PU-4180 Pump, LC-NetII/ADC Interface Box, CO-4060 Column Oven, MD-4010 Photodiode Array Detector, ChromNAV v. 2.2.8.5 software) in a C_{18} column (Waters Symmetry, 5 μm, 3.9 mm × 150 mm), using ACN/H_2O

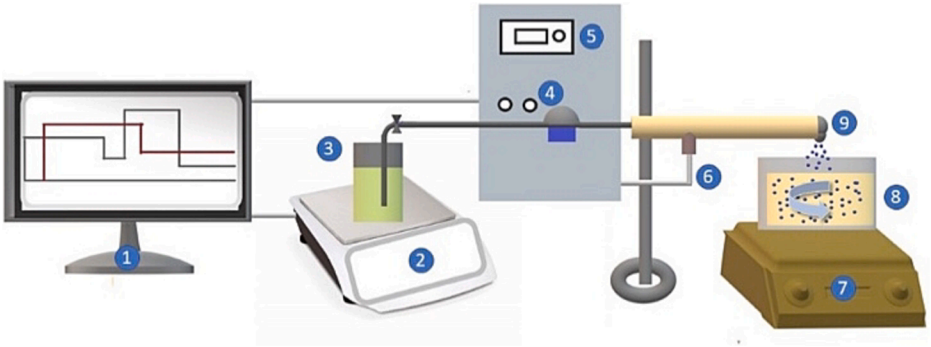

Fig. 1. Setup for alginate hydrogel microsphere production in compressed air-assisted spraying equipment. The experimental tests were followed via the cockpit in the screen of the equipment (1). 20 mL of alginate solution (3) was injected into a silicone tube after being weighed in the balance (2). Pump speed (4) and air flow rate (5) were the processing parameters. The flow of alginate solution was controlled by the speed pump, while air flow rate (6) was controlled at the nozzle (9) injecting the solution into a gelation bath (200 mL of 150 mM $CaCl_2$) (8) resulting in alginate hydrogels. Mechanical stirring of the bath (7) was set at 500 rpm.

Table 1
Experimental conditions (air flow rate and pump speed) used for the preparation of alginate aerogels by the compressed air-assisted prilling gelation method. Particle diameter is expressed as average mean diameter (and standard deviation).

Aerogel sample	Air flow (L/min)	Pump speed (rpm)	Particle diameter (μm)
1	30	750	107 (144)
2	30	300	98 (126)
3	35	750	57 (38)
4	35	300	75 (50)
5	40	750	44 (27)
6	40	300	47 (22)
7	45	750	45 (28)
8	45	300	41 (45)
9	50	750	37 (23)
10	50	300	40 (23)

(65:35 % v/v) mixture as the mobile phase (1.4 mL/min flow rate) at 30 °C, with a run time of 7 min and retention time of 2.7 min. The injection volume was 25 μL and the UV-detector wavelength was 254 nm. Stock standard solutions of BDP in ACN:H_2O (65:35 % v/v) were prepared at room temperature. Samples were micro-filtered before HPLC analysis. The calibration curve of BDP in the ACN: H_2O (65:35 % v/v) mixture was obtained and validated ($R^2 = 0.9998$) from triplicate serial dilutions over the concentration range of 1–80 μg/mL.

The equation for calculating the loading yield is expressed as follows [24]:

$$\text{Drug loading} = \frac{m_{BDP}}{m_{BDP-\text{loaded alginate aerogels}}} x\,100 \quad (1)$$

2.5. Physicochemical and structural characterization of aerogels

Scanning electron microscopy (SEM EVO LS15, Zeiss, Oberkochen, Germany) was used to evaluate the size of the alginate aerogel particles. The external morphology of BDP-loaded alginate aerogels was imaged using a Scios 2 SEM instrument (ThermoFisher Scientific, Waltham, MA, USA) with an accelerating voltage of 2 kV. A vacuum-resistant carbon tape was used to fix the samples. Sputter coating was not applied here in order to avoid changes in the morphological characteristics [25].

The textural properties of the pristine and the loaded alginate aerogels were assessed with a Quantachrome Nova 3000e surface area and porosity analyzer (Quantachrome Instruments, Graz, Austria). For degassing, vacuum (*ca.* 1 Pa) was applied at 60 °C for 24 h before analysis. BET and BJH methods were used to determine the surface area, pore size distribution and specific pore volume.

The compressibility of alginate aerogels were measured by using a graduated cylinder. Alginate aerogels were placed inside a graduated cylinder, and their initial volume (V_0) was measured. The graduated cylinder was tapped at a rate of 30 strokes per minute until a constant volume was reached, and the final tapped volume (V_{tapped}) was measured. Compressibility (%) was then calculated using the following equation [23]:

$$\text{Compressibility} = \left(\frac{V_0 - V_{tapped}}{V_0}\right) x\,100 \quad (2)$$

Attenuated total reflection (ATR) IR spectroscopy was performed on BDP, alginate powder, unloaded alginate aerogel particles, BDP-loaded alginate aerogel particles, and the physical mixture of BDP and alginate aerogels on a diamond crystal in a PerkinElmer Spectrum Two FTIR spectrometer (PerkinElmer, Waltham, MA, USA) in the 4000–400 cm^{-1} wavenumber range based on 8 scans at a resolution of 2 cm^{-1} and using air as background. The CAMO Unscrambler X software (CAMO Analytics AS, Oslo, Norway) was used to analyze the data.

The XRPD patterns of BDP, alginate powder, unloaded alginate aerogel particles, BDP-loaded alginate aerogel particles, and the physical mixture of BDP and alginate aerogels were recorded in the range from 10 to 80° (2Θ) in steps of 0.03° with a Rigaku Smartlab diffractometer (Rigaku, Tokyo, Japan) operating at 45 kV and at 200 mA with CuK_α radiation (1.54056 Å).

Differential scanning calorimetry (DSC) analysis was carried out using 2 mg of each sample in a non-hermetically sealed aluminum pan using a DSC Q100 equipment (TA Instruments, New Castle, DE, USA). An empty aluminum pan was the reference. The specimens were heated from 25 to 300 °C at a constant heating rate of 10 °C/min under a N_2 flow of 50 mL/min.

2.6. Simulated lung deposition tests

The *in vitro* aerodynamic deposition of BDP-loaded alginate aerogel particles was measured using a NGI impactor (Copley, Nottingham, UK). A mouthpiece adapter was used corresponding to a single-dose dry powder inhaler device. The NGI contained seven stages and a micro-orifice collector (MOC). Before the analysis, the stages of the impactor were treated with a 1 % (w/v) solution of glycerin in methanol to prevent inhaled particles bounce back and maintain particle stability inside the impactor. The used inhaler device had low resistance (pressure drop across the device is lower than 5 $Mbar^{0.5}$L/min, i.e., Aerolizer or Breezhaler) [26]. The vacuum pump was operated at a flow rate of 100 L/min for 2.4 s, responding to a pressure drop behind the impactor of 4 kPa and 4 L of air volume, in accordance with the European Pharmacopeia [9]. Based on the manufacturer's calibration, the Da50 aerodynamic cut-off distance for each NGI stage was as follows: stage 1 (6.12 μm), stage 2 (3.42 μm), stage 3 (2.18 μm), stage 4 (1.31 μm), stage 5 (0.72 μm), stage 6 (0.40 μm), and stage 7 (0.24 μm). The nearest cut-off limit to 5 μm for NGI was stage 2 (3.42 μm).

The collected particles were extracted from every stage of the impactor with an ACN:H_2O (65:35 % v/v) solution and then the amount of BDP in each stage was determined by HPLC (cf. Section 2.4). *In vitro* aerodynamic properties were represented by the mass median aerodynamic diameter (MMAD), emitted fraction (EF), and fine particle fraction (FPF). MMAD specifies the particle diameter where 50 % of its cumulative weight is undersized. EF represents the percentage of drug recovered in the NGI, and FPF indicates the fraction of emitted dose whose aerodynamic size is less than 5 μm.

2.7. In vitro drug release studies

The *in vitro* release of BDP from the loaded alginate aerogels was investigated by two different methods, as follows.

Long-term release tests were carried out using a dialysis bag [27,28]. BDP-loaded alginate aerogel particles (*ca.* 10 mg) containing *ca.* 450 μg of the active compound (4.5 % w/w loading) were sealed within a dialysis bag (MWCO = 12,400 Da), which also contained 1.0 mL solution of PBS pH 7.4 with 20 % v/v methanol. The inclusion of methanol was necessary to overcome the solubility challenges associated with the drug [28]. The dialysis bag, along with its contents, was then placed inside a plastic container filled with 15 mL of the same solvent, and the entire system was maintained at a constant temperature of 37 °C. Continuous agitation at a rate of 100 rpm ensured mixing. At specified time intervals, aliquot samples (300 μL) were extracted from outside of the dialysis bag for analysis, and an equivalent volume of fresh medium was introduced. The collected aliquots were then analyzed by HPLC (cf. Section 2.4). The measurements were run in triplicate. The solubility of BDP was also determined in the PBS pH 7.4 with 20 % v/v methanol at 37 °C.

The first fast part of the drug release process was also investigated under the same conditions (using PBS pH 7.4 with 20 % v/v methanol as the release medium at 37 °C under constant stirring), but using on-line UV–Vis detection based on a previously published fast kinetics method [29,30]. The experiments were carried out in a standard spectrophotometric quartz cuvette (1.00 cm x 1.00 cm) in the thermostated sample holder of a diode array UV–Vis spectrophotometer (Agilent Technologies, Santa Clara, CA, USA). First, the BDP-loaded alginate aerogel (*ca.* 1.0–1.5 mg with *ca.* 70–105 μg BDP content) was weighted into the dry cuvette, and 3.0 mL release medium was added. Detection was started immediately, and the UV–Vis spectrum of the liquid phase was recorded on-line at high time resolution. These time-resolved UV–Vis spectrum series were characteristic for the dissolved BDP in the release medium. The time-dependent concentration of dissolved BDP was calculated from the absorbance measured at the wavelength of 242 nm after correcting the baseline using the double-wavelength method [29,30]. The measurements were run in triplicate.

The first part of the drug release process was modelled based on the work of Hirai et.al. [31]. Their kinetic model accounts for the fast dissolution of amorphous drug deposits at the solid–liquid interface and also takes into account the slower formation and precipitation of stable crystals under non-sink conditions. Therefore, the temporary improvement in apparent drug solubility can be quantified. The following equation describes such drug release profiles.

$$C_b = C_S[1-\exp(-k_D t)] + \frac{k_D(C_M - C_S)}{k_D - k_C}[\exp(-k_C t) - \exp(-k_D t)] \quad (3)$$

where C_b is the time-dependent concentration of the dissolved drug in the release medium, C_M is the apparent solubility of the amorphous drug, and C_S is the solubility of the stable crystalline drug. The kinetic parameters are the pseudo first-order rate constant of the dissolution of the amorphous drug (k_D), which also incorporates the total starting amount of the drug formulation; and the first-order rate constant of the crystal precipitation process (k_C). The physicochemical background of the model and the elaboration of the kinetic considerations are given in the original article [31].

2.8. Characterization of hydrated aerogels

NMR relaxometry measurements were performed with a Minispec Bruker mq20 relaxometer instrument (Billerica, MA, USA). The NMR tubes were filled with unloaded alginate aerogel particles or with BDP-loaded alginate aerogels. Hydrated samples were obtained by adding liquid water in multiple aliquots. Mild sonication was used in a bath for 15 min for homogenizing the hydrated aerogels, followed by prolonged equilibration for 24 h. All measurements were performed at 6 dB [31–33]. T_2 (spin–spin) relaxation times were determined in all samples based on the CPMG (Carr-Purcell-Meiboom-Gill) sequence using various echo times (0.08, 0.12, and 0.16 ms). Different relaxation domains arise for water in the porous samples depending on the chemical environment around the water molecules. The MERA (Multi–Exponential Relaxation Analysis) algorithm was used under MATLAB v.10.0 (MathWorks Inc., Middlesex County, MA, USA) to determine the exponential decays in the primary CPMG decays corresponding to the different relaxation domains [32].

2.9. In vitro cytotoxicity test

The NIH-3 T3 cell line (ATCC: CRL-1658) was cultured in DMEM medium supplemented with 10 % bovine calf serum and 1 % penicillin–streptomycin, maintaining a 37 °C temperature in a humidified atmosphere with 5 % CO_2 [33,34]. When the confluence was *ca.* 60–70 %, the culture medium was removed, and the cells were washed with PBS. Then cells were trypsinized, and cell counts were determined using Vi-CELL XR (Beckman Coulter, California, USA). The resulting cell suspension was diluted to achieve the desired cell concentrations and the cells were seeded in 24-well plates at 12,000 cell/cm^2 for 24 h and 8000 cells/cm^2 for 48 h.

These cell cultures were maintained at 37 °C in a humidified 5 % CO_2 atmosphere for 24 h and subsequently treated with samples (alginate aerogels and BDP loaded alginate aerogels obtained through $scCO_2$ impregnation with 5 % vol. acetone as a co-solvent) in triplicate. All samples were sterilized under UV-light for 30 min before introducing into 24-well inserts (PET membrane, 0.4 μm pore size). The inhaled formulation contained 1 μM of BDP, with the amount of alginate

aerogels equating to that without BDP (*ca.* 11.7 mg). The inserts were introduced on the cell culture plate, 100 μL of culture medium was added on top of the inserts and negative controls and the plates were maintained at 37 °C in a humidified 5 % CO_2 atmosphere for 24 and 48 h.

Non-treated cells were employed as the negative control group. Cell viability assessments at 24 and 48 h post-treatment utilized the resazurin assay, where the nonfluorescent blue dye, resazurin, underwent conversion to its fluorescent form, resorufin, in response to metabolically active cells [35].

Following treatment, the inserts containing BDP-loaded alginate aerogels and alginate aerogels were removed, and the medium in the plates was aspirated. Subsequently, 300 μL of resazurin solution (44 μM) was added to the plates, which were then incubated for 3 h at 37 °C, 5 % CO_2, 95 % humidity, and shielded from light. Fluorescence measurements were conducted using the Infinite M1000 Pro (Tecan, Männedorf, Switzerland) with an excitation wavelength of 544 nm and an emission wavelength of 590 nm.

2.10. Ex vivo bronchial permeability tests

2.10.1. Ex vivo permeability tests

Bronchial permeability experiments were conducted with the BDP-loaded alginate aerogel particles (25 mg with 6 % w/w BDP loading). The test was also carried out using an equivalent amount of microcrystalline BDP (1.5 mg) for comparison.

The lung of a freshly sacrificed domestic pig was obtained from a local slaughterhouse and transported in a polystyrene box to the laboratory. Subsequently, the intact tracheobronchial tree was carefully isolated with a scalpel, scissors, and tongs and visually examined to confirm the absence of any damage to the epithelial surface of the bronchial tissue such as cuts or cracks. Next, the main and secondary bronchi were cut into uniform small pieces capable of completely covering the area available for permeation of the Franz cells (0.785 cm^2). The pieces were washed in 0.9 wt% NaCl solution at room temperature with successive changes of medium until no blood was visible in the liquid medium. The bronchial tissue pieces were immersed in NaCl 0.9 wt% and kept there at 4 °C for *ca.* 12 h. The stability of the tissue in the receptor medium was examined prior to conducting the permeability tests.

The tissue pieces were fitted into vertical diffusion Franz cells with the basement membrane tissue pointing to the receptor compartment. The bronchial curvature was not preserved during the experiment due to the design of Franz cells and to ensure proper contact between the tissue and the liquid in both the donor and the receptor chambers. The donor (2 mL) and receptor (6 mL) chambers were filled with the previously described PBS/MeOH medium ensuring the absence of any bubbles, and maintained at 37 °C under 100 rpm. After 30 min of equilibration, the medium of the donor chambers was removed and replaced by the samples (i.e., BDP-loaded alginate aerogels or pure BDP) immersed in 500 μL of PBS/MeOH medium. The donor chambers were sealed with parafilm to avoid evaporation. For analysis, 1 mL of the medium was taken every hour from the receptor chamber and replaced with 1 mL of fresh medium, taking care to remove any bubbles from the diffusion cells. BDP content in the aliquots was determined by HPLC (cf. Section 2.4). The tests were carried out for a duration of 3 h for all formulations in triplicate.

2.10.2. IR-Raman analysis of the lung tissue

After the permeability tests were completed, the rest of the formulation remaining on the surface of the bronchial tissues was carefully removed with a spatula. The recovered tissues were carefully washed by immersion in distilled water to eliminate the rest of the drug that had not penetrated into the bronchial tissues. All recovered bronchial samples were visually inspected to confirm that none of them had cracks or other modifications.

The tissues were stored in Petri dishes at −80 °C until analyzed by IR-Raman Spectroscopy (WITec, alpha 300 R, Wissenschaftliche Instrument und Technologie GmbH, Ulm, Germany). The IR-Raman study involved a line scan conducted in the x-z plane. The excitation wavelength was 532 nm, and the laser power was 1.2 mW. Each data point was measured with 100 accumulations, using an integration time of 1.0 s, and observed through a 50X objective lens (Zeiss LD EC Epiplan-Neofluar Dic 50×/0.55). The analysis was focused on two distinct regions within the tissue specimens. The first region was the region extending from epithelial surface, positioned at a depth ranging from 6.5 to 15.6 μm. The second region is the basement membrane which encompasses the lower segment of the tissue. A peak at the wavelength of 1345 cm^{-1} present in the spectrum of the tissue was utilized as a reference for the quantification of BDP in the tissue. The ratio of the peak associated with BDP at 1666 cm^{-1} to that of the reference peak of tissue was determined for each of the differently treated tissue samples.

2.11. Statistical analysis

All data were expressed as mean ± standard deviation. Statistical analyses of drug loading results were performed using one-way ANOVA with post-hoc Tukey HSD test using GraphPad Prism Software (San Diego, CA, USA).

3. Results and discussion

3.1. Optimization of alginate aerogel production by prilling gelation

The process adjustment of the prilling gelation method (Section 2.2) was carried out to accommodate aerogels production, specifically to optimize the size of particles needed for the delivery of drugs by inhalation. The method was additionally optimized to obtain uniform and spherical alginate aerogel particles. Air flow rate and pump speed were used as the main processing parameters. Prior to adjusting air flow rate and pump speed, the concentration of the alginate solution was screened. Low concentrations of alginate (less than 1.5 % w/v) failed to preserve the spherical shapes of the gel particles, likely due to the incomplete crosslinking of alginate. Increasing the concentration above 2 % w/v resulted in clogging of the nozzle [36]. Accordingly, the alginate concentration of 1.75 % w/v was selected as a trade-off value to maintain the particle shape and to ensure a stable fluid flow through the nozzle. A solvent exchange with ethanol was carried out to facilitate the supercritical drying process. Compared to conventional powder technologies (jet milling, wet milling, spray drying), using $scCO_2$ is more cost-effective and can reduce organic solvent consumption.

SEM imaging and digital image analysis were conducted after supercritical drying to examine the effects of air flow rate and pump speed on the shape and size of aerogel particles (Fig. 2). The pump speed had no significant impact on particle size as there was no significant difference when the same air flow rate and different pump speeds were used.

Generally, an increase in air flow rates resulted in a decrease in average particle size. In the nozzle, compressed air divided the flowing alginate solution into fine droplets, thus greatly affecting the particle size. Noteworthy reductions in average particle size were observed when

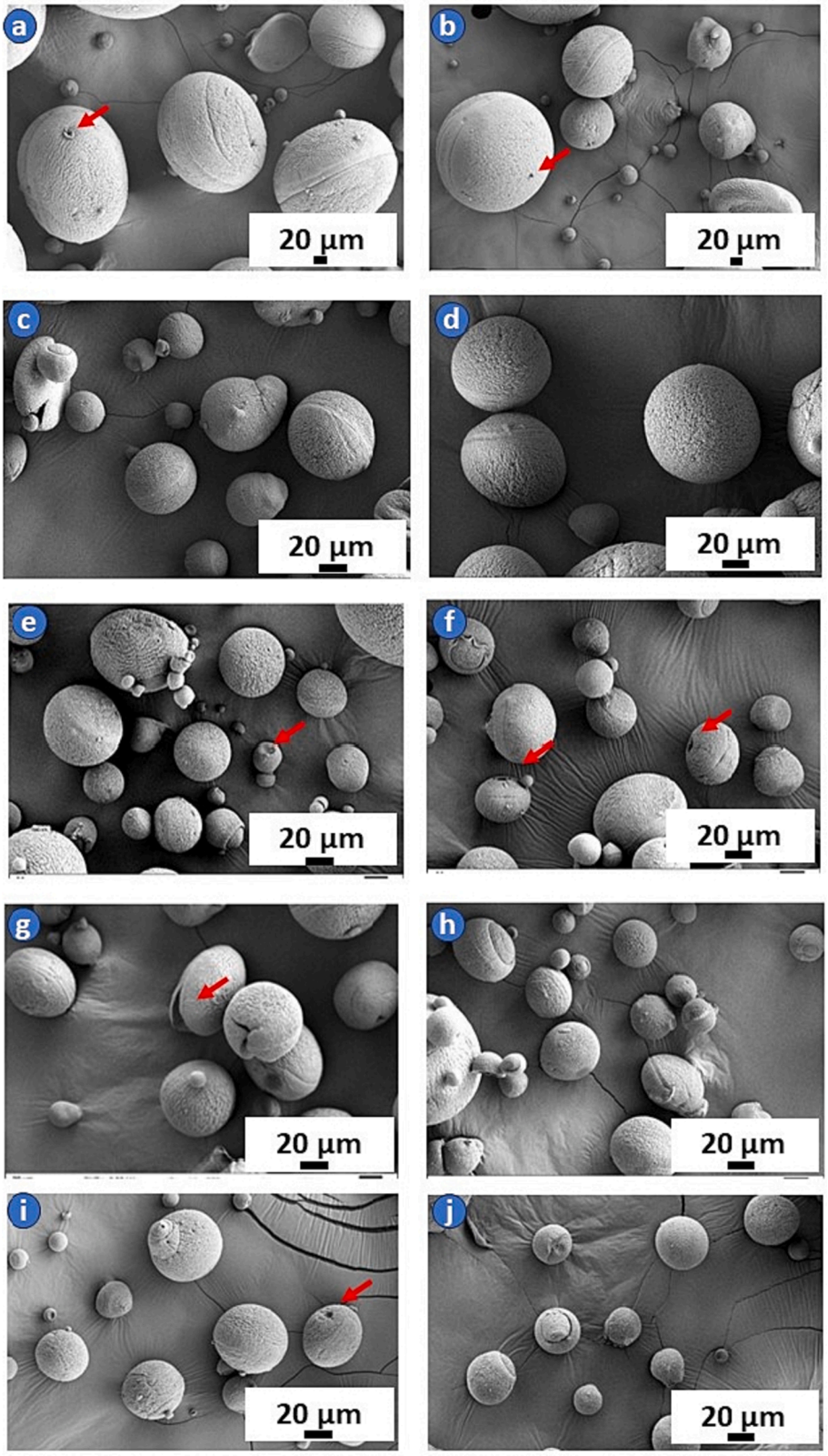

Fig. 2. SEM images of alginate aerogels obtained by prilling using different air flow rates and pump speeds: (a) sample 1 (30 L/min, 750 rpm); (b) sample 2 (30 L/min, 300 rpm); (c) sample 3 (35 L/min, 750 rpm); (d) sample 4 (35 L/min, 300 rpm); (e) sample 5 (40 L/min, 750 rpm); (f) sample 6 (40 L/min, 300 rpm); (g) sample 7 (45 L/min, 750 rpm); (h) sample 8 (45 L/min, 300 rpm); (i) sample 9 (50 L/min, 750 rpm), (j) sample 10 (50 L/min, 300 rpm). Red arrows indicate the presence of holes in certain aerogel particles. (For interpretation of the references to color in this figure legend, the reader is referred to the web version of this article.)

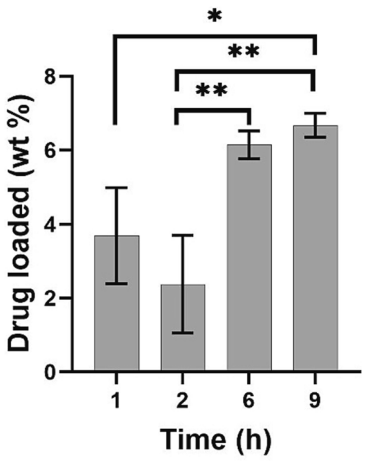

Fig. 3. BDP loading in alginate aerogel particles using different impregnation times (1, 2, 6, 9 h) at 65 ^{0}C, 215 bar and in $scCO_2$ with acetone as co-solvent (5 % vol.). * $p < 0.05$ and ** $p < 0.01$.

the air flow rates were increased from 30 to 40 L/min. Significant differences ($p < 0.01$) were detected with the same pump speed at different air flow rates of 30 and 35 L/min (samples 1–2, samples 3–4) in comparison to samples obtained from higher air flow rates (samples 5–6, samples 7–8, samples 9–10) (Table 1 and Fig. 2). However, starting from a flow rate of 40 L/min (40, 45 and 50 L/min), although there was a decline in average particle size with increasing air flow rate, the reduction was not significant. The reason can be that from the air flow rate of 40 L/min, the atomization and shear forces might have almost reached their maximum efficacy.

Aerogel particles obtained at a low air flow rate tended to have a hole at the top (red arrows in Fig. 2). This tendency is explained by the failure of the low compressed air flow rate to remove bubbles from the alginate solution. Consequently, when alginate droplets containing bubbles got in contact with the $CaCl_2$ solution, the bubbles were released, causing a hole to form. Sample 9 (air flow rate: 50 L/min, pump speed: 750 rpm) was selected to be loaded with BDP due to its advantageous diameter (*ca.* 37 μm) and low production variability.

3.2. BDP-loading into alginate aerogel particles

The solubility of BDP in $scCO_2$ is extremely low [37]. Following previous impregnation tests (not showed), $scCO_2$ was amended with an organic solvent (acetone) as a co-solvent to increase its solvation power leading to higher BDP loadings [24]. The BDP loading yield was affected by the contact time during the $scCO_2$ impregnation process (Fig. 3). During the first hours of impregnation (1 and 2 h), aerogels had a similar BDP content, but with high variability. The equilibrium state was not reached in such short time and may explain this phenomenon. After 6 h, the loading yield was similar to those obtained after 9 h, indicating the completion of the process. Drug loading obtained from $scCO_2$ impregnation varies with choices in drugs, carriers, and experimental conditions [24]. To the best of the authors' knowledge, there is no literature available on BDP impregnation into aerogels but, as an example, nimesulide impregnation into hydrophilic silica aerogels shows a maximum loading of 1.53 wt.% under specific conditions (210 bar and 60 °C) [38,39].

The initial weight ratio between BDP and alginate aerogels was kept at 1:10 in all loading experiments. Therefore, the *ca.* 7 wt% loading means a *ca.* 75 % efficiency relative to the initial drug amount, despite the low solubility of the drug in pure $scCO_2$ [37]. The high loading efficiency is mainly attributed to the right choice of the co-solvent. Compared to current commercial DPIs, a much higher drug-to-excipient weight ratio was achieved in this work: Fostair NEXThaler 200 μg/6 μg contains 206 μg BDP/formoterol fumarate dihydrate and 9.8 g lactose monohydrate [40], and Seebri® Breezhaler® 44 μg inhalation powder contains 63 μg glycopyrronium bromide and 23.6 mg lactose [41]. Hence, there might be a positive impact on patients due to a higher drug-to-excipient ratio, as they would inhale less that reduces the burden of inhaling, and still achieve the therapeutic levels. Additionally, the cohesive forces between the particles in current commercial high dose inhaled formulations are high requiring high flow rates for appropriate dispersion [42]. The present aerogel formulations can be beneficial for patients who have difficulties inhaling high flow rates due to their pathologies. Overall, inhaled formulations produced by $scCO_2$ impregnation could provide a feasible and convenient method of achieving a high-dose drug delivery system.

Table 2
Specific surface area (A_{BET}), pore volume ($V_{p,BJH}$) and mean pore diameter ($d_{p,BJH}$) of alginate aerogels and BDP-loaded alginate aerogels obtained after 9 h of $scCO_2$ impregnation.

Formulation	A_{BET} (m^2/g)	$V_{p,BJH}$ (cm^3/g)	$d_{P,BJH}$ (nm)
Blank aerogels (sample 9)	351 ± 17	3.6 ± 0.2	37.0 ± 1.8
BDP-loaded aerogels (9 h)	299 ± 15	3.1 ± 0.2	31.0 ± 1.6

3.3. Solid state characterization of BDP-loaded alginate aerogels

The obtained aerogel particles have high specific surface areas, the pores are mainly in the mesoporous range (Table 2) and the pore size distribution of alginate aerogels is unimodal (Fig. S2 in the Supporting Information). SEM images of aerogels were taken after supercritical drying and after $scCO_2$ impregnation (Fig. 4). In all cases, the particles obtained by $scCO_2$ impregnation had a spherical shape with high surface roughness due to the mesopores.

Materials with smooth and clean surfaces typically exhibit higher surface energy [4]. However, when these materials are combined with substances featuring greater surface roughness, there is a potential decrease in surface energy. This reduction in surface energy resulted in higher distances between particles, thereby enhancing particle dispersion. Consequently, cohesive forces between particles strongly influenced flowability and fluidization [43]. In terms of flowability, the compressibility (%) was employed to express the solid flow properties of alginate aerogel particles. A compressibility range of 5–15 % indicates excellent flowability, while 12–18 % suggests good flowability [23]. Following triplicate measurements, the calculated compressibility of alginate aerogels was found to be 15.8 ± 1.6 %, suggesting that alginate aerogels with high surface roughness exhibit good-to-excellent flow properties. This characteristic makes them promising candidates for use in pulmonary drug delivery.

An XRD analysis was performed on BDP-loaded aerogel formulations to elucidate their crystalline state (Fig. S3 in Supporting Information). Sharp and intense peaks at 11.28, 14.44, and 20.06° 2θ angles are typical of crystalline BDP [44]. None of the BDP-loaded alginate aerogel formulations displayed these peaks indicating that the drug remained in the amorphous state after impregnation. The XRD patterns of the physical mixtures of BDP and alginate aerogels revealed the intensive peaks of BDP. Hence, the amorphous state of BDP after loading in the alginate aerogels can be attributed to the applied $scCO_2$ impregnation technique. The solvent impregnation method utilizing $scCO_2$ was previously reported to be a feasible method for the amorphization of various drugs in porous materials [24,45,46].

The IR spectra of BDP, BDP-loaded alginate aerogels (9 h), pristine alginate aerogel and bulk sodium alginate are shown in Fig. S4 in Supporting Information. Physical mixtures of BDP and alginate aerogels corresponding to the minimum (2.4 wt%) and maximum (6.7 wt%) content of BDP in alginate aerogels were also analyzed for the sake of comparison. Sodium alginate (Fig. S4b) was clearly identified via the asymmetric and symmetric C=O vibrations at 1590 and 1400 cm^{-1} and a broad band at 3400 cm^{-1}, corresponding to the presence of hydroxyl

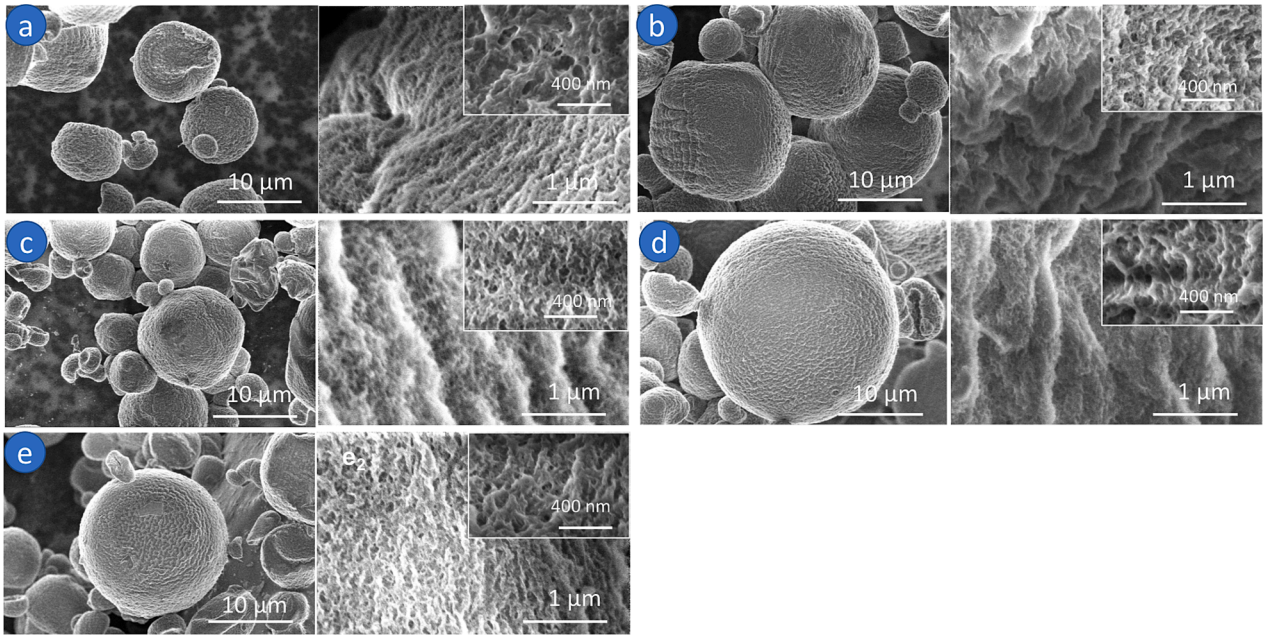

Fig. 4. SEM images at different magnifications of (a) pristine alginate aerogels (sample 9) and BDP-loaded alginate aerogels obtained using different contact times in impregnation: (b) 1, (c) 2, (d) 6, and (e) 9 h.

Table 3
In vitro aerodynamic properties of BDP-loaded alginate aerogels.

	Contact time for drug impregnation (h)			
	1	2	6	9
MMAD (µm)	3.7 ± 0.1	3.3 ± 0.1	2.9 ± 0.9	3.3 ± 1.4
EF (%)	99.0 ± 0.7	98.0 ± 0.1	98.0 ± 0.1	99.0 ± 0.3
FPF (%)	68.0 ± 0.7	70.0 ± 0.9	71.0 ± 0.8	72.0 ± 2.8

groups [47,48]. Compared to bulk sodium alginate, the ionic binding between the COO^- group and Ca^{2+} in the alginate aerogels is indicated via the distortion of the asymmetric $–COO^-$ stretching band at 1590 cm^{-1}.

The IR spectrum of BDP showed conjugated and non-conjugated C=O stretching bands at 1724 and 1658 cm^{-1}, respectively [44,49]. C=C stretching band was exhibited at 1615 and 1608 cm^{-1} and C-O bands were shown at 1186 cm^{-1}. Compared with the spectra of alginate powder and alginate aerogel, the spectra of BDP-loaded alginate aerogels revealed C=O stretching band at 1735 cm^{-1} (asterisks in Fig. S4), which verified the presence of BDP. The C=O stretching band was clearly visible in the IR spectra of the physical mixtures with different BDP contents.

In the IR spectrum of BDP-loaded alginate aerogels, there is an ester carbonyl stretching band at 1735 cm^{-1} suggesting the interaction between the carbonyl group of BDP and the hydroxyl group of alginate. The intermolecular interactions between BDP and alginate are additional explanations for the good loading yield [22,50].

The DSC thermograms of BDP, along with that of alginate aerogel formulations and mixtures of BDP and alginate aerogel are shown in Fig. S5 in Supporting Information. Pure BDP showed a sharp endothermic event around 212.5 ^{0}C, which corresponds to its melting temperature. In physical mixtures, alginate and BDP were clearly shown to independently cause thermal events. However, when BDP was loaded into alginate aerogels, the typical melting event of BDP could not be observed, which is a further evidence for its amorphous state.

3.4. *In vitro* aerodynamic deposition of BDP-loaded alginate aerogels

A NGI impactor was used to test the aerosol performance of the BDP-loaded aerogel formulations. As a result of their high porosity, the MMAD values of the aerogel particles (Table 3) are *ca.* 12-fold smaller than their geometric particle sizes (Table 1). Particles with MMAD in the 1–5 µm range generally settle in the bronchioles and alveoli, which is the target area in pulmonary drug delivery [1,9,51].

The EF and FPF values of all formulations (Table 3) were high (from 98 % and 68 %, respectively), indicating good flowability and deep lung penetration. The high EF results also indicate that the acetone co-solvent was effectively removed, and the impregnated aerogels are free of solvents.

The majority of the BDP content of the loaded aerogel particles was deposited during the first stage of the impactor, and drug content diminished gradually over the subsequent stages (Fig. 5). The drug content was practically zero in the last stages, indicating the majority of BDP can be delivered to the bronchioles and bronchi of the respiratory system, which is suitable for local treatment.

Particles with a geometric diameter above 5 µm and low tapped density (<0.4 g/cm^3) may have an aerodynamic diameter smaller than 5 µm which are suitable for inhalation formulations [52]. This relationship could be explained by Stokes equation [53]:

$$d_a = d_g \cdot \sqrt{\frac{\rho_p}{\chi}} \quad (4)$$

where d_a is the aerodynamic diameter, d_g is the geometric diameter, ρ_p is the bulk density, χ is the dynamic shape factor.

Alginate aerogels from compressed air-assisted spray gelation and supercritical fluid drying exhibit high porosity, and a geometric size of *ca.* 38 µm with an aerodynamic size below 5 µm. Hence, inhaled formulations based on alginate aerogels as large porous particles hold promise for pulmonary drug delivery.

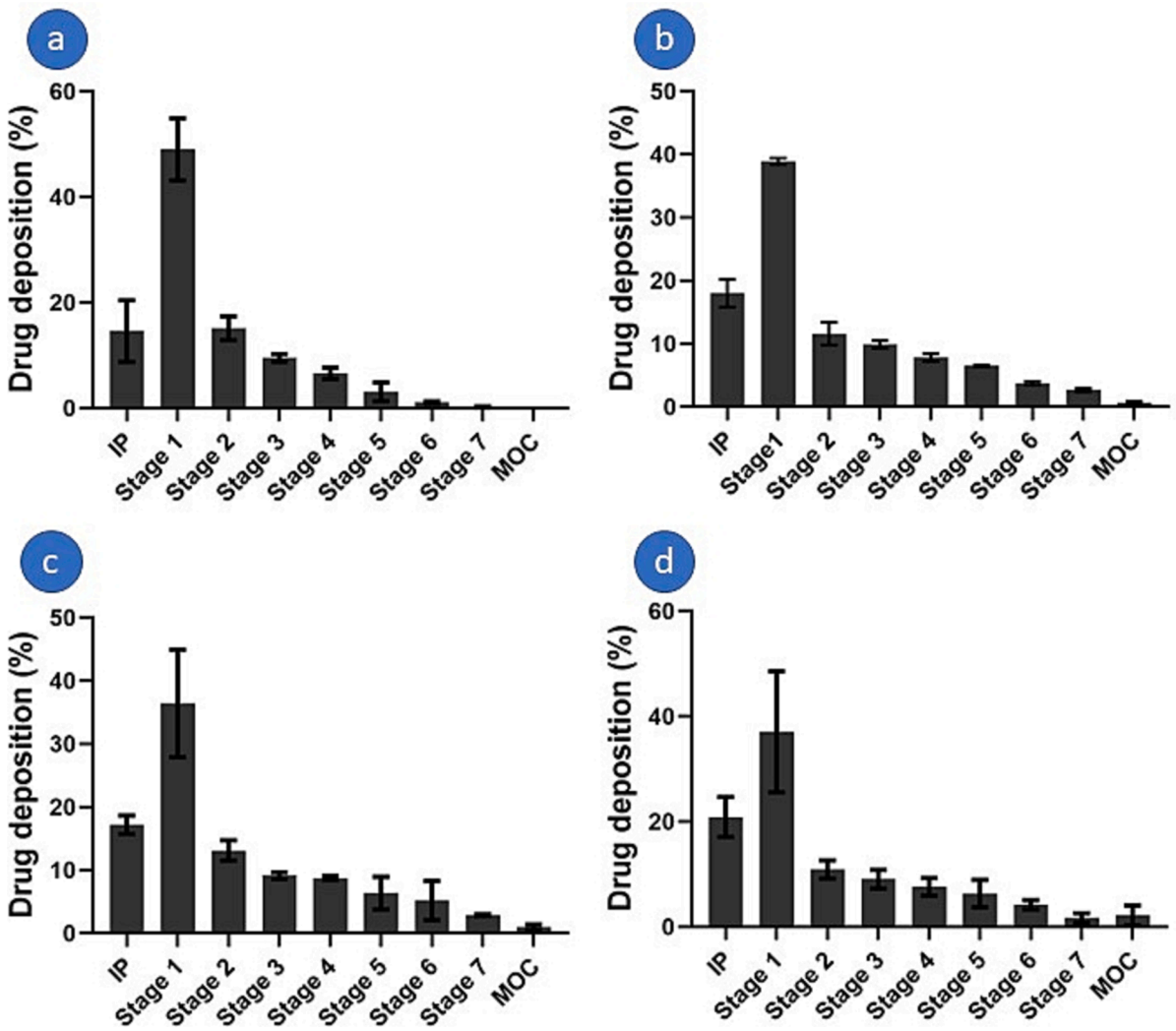

Fig. 5. Drug deposition profiles of BDP-loaded alginate aerogel microparticles prepared using different contact times for drug impregnation: (a) 1, (b) 2, (c) 6, and (d) 9 h.

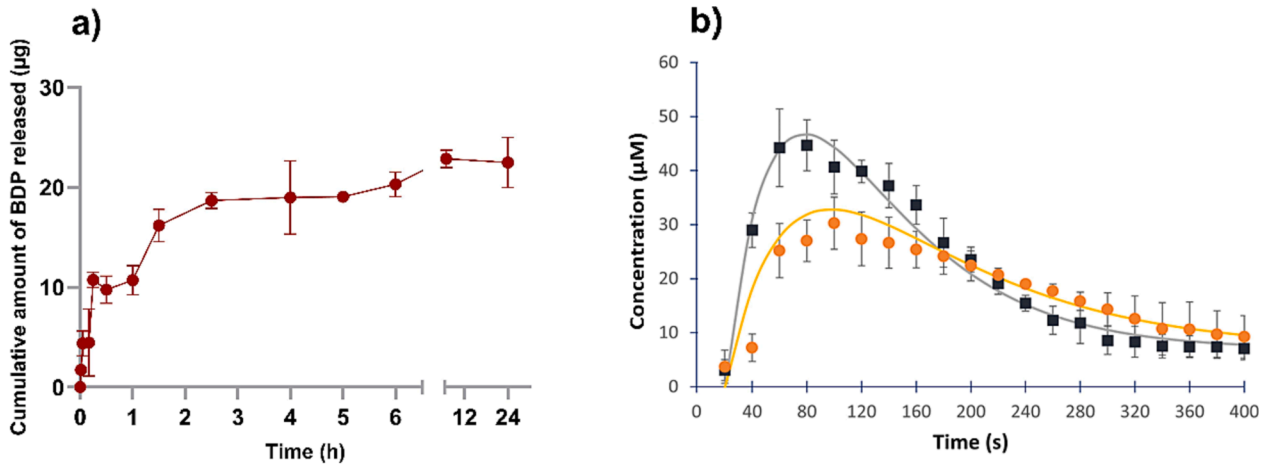

Fig. 6. (a) *In vitro* release profile (n = 3) of BDP from alginate aerogel carriers in PBS pH 7.4 with 20 % methanol (37 °C, 100 rpm) measured by the classical dialysis method. (b) Drug release profiles (n = 3) of different amounts of BDP-loaded alginate aerogels in the same medium measured by a fast kinetics method. Curved lines correspond to the simulated drug release profiles based on the kinetic model developed by Hirai et.al. and summarized in eq. (3) in Section 2.7 [31]. Symbols: black squares and gray line: experimental and simulated data of 1.5 mg BDP-loaded alginate aerogels, respectively; orange circles and yellow line: experimental and simulated data of 1.0 mg BDP-loaded alginate aerogels, respectively. (For interpretation of the references to color in this figure legend, the reader is referred to the web version of this article.)

3.5. Drug release studies of BDP-loaded alginate aerogels

The drug release results obtained by the classical dialysis method [54] are shown in Fig. 6a. The BDP-loaded alginate aerogels exhibited a release pattern characterized by two distinct phases. First, a sudden (burst) release of BDP took place during the initial 10 min, followed by a slow and sustained release. The process is controlled by the limited solubility of the drug, which was measured to be 4.3 μg/mL in the release medium (PBS pH 7.4 containing 20 % methanol) at 37 °C. Sink conditions did not apply in this experiment, and additionally, the alginate carrier formed a hydrogel in the longer term, which did not dissolve during the 48-hour test.

As discussed in the next section, the observed burst in the first phase of the release kinetics can be explained by the fast and facile hydration of the porous alginate carrier in the aqueous medium, which instantly repels the lipophilic BDP initially covering the surface of alginate aerogel backbone [11]. However, the instantaneously released drug can precipitate from the release medium and bind to the dialysis membrane. Furthermore, the highly hydrophilic nature of the alginate aerogels leads to microscopic swelling that ultimately collapses the pore structure of the aerogel. As a result, part of the BDP can be trapped or re-absorbed in the formed dense hydrogel. In the longer term, these effects ultimately limit the amount of the dissolved drug in the release medium.

Lastly, the distinct physicochemical properties of the lung, including the presence of lung surfactants (mixture of phospholipids, neutral lipids, and proteins) and the lipophilic nature of the lung epithelial wall, pose significant challenges when compared to the semipermeable membranes and aqueous release medium commonly employed in *in vitro* testing [55,56]. BDP is a lipophilic compound with a log*P* value of 3.49, indicating that it primarily undergoes passive transcellular diffusion when crossing epithelial barriers [57,58]. However, during the *in vitro* test, the selected aqueous release medium and semipermeable membrane did not provide conducive conditions for facilitating BDP diffusion.

Fast kinetics experiments were conducted to further study the first part of the drug release process. Typical release curves measured by this method are shown in Fig. 6b. The detected time resolved UV–vis spectra unambiguously show the prompt appearance of high concentrations of BDP in the release medium, which is followed by the steady depletion of the dissolved drug. The maximum concentration of dissolved BDP was 45 μM when 1.5 mg of loaded aerogel was agitated in 3 mL release medium. This concentration is *ca.* 10 times higher than the solubility of crystalline BDP (4.6 μM) under the applied conditions. The maximum concentration was reached in *ca.* 1 min and maintained for an additional *ca.* 3 min. The drug concentration then decreased because of the recrystallization and precipitation of BDP from the supersaturated solution (nano-dispersion). The release profile of 1.0 mg of BDP-loaded aerogels showed a similar pattern. Overall, the alginate aerogel particles proved to be effective solubilizing aids for the low water solubility drug under the applied non-sink conditions. Based on literature precedents, delivery efficiency can be characterized in such cases by the apparent supersaturation concentrations and the duration to reach and maintain these supersaturated concentrations [31,59,60].

The enhanced solubilization and the special drug release profiles can be explained by the amorphization of BDP on the pore walls of the alginate aerogels as a result of adsorptive precipitation following the evaporation of the solvent in the supercritical fluid-assisted impregnation. The physical basis of this amorphization method is well-described in the literature [24,59,60]. In the case of the alginate aerogels, the hydration of the carrier and the repulsion of the amorphous drug from the alginate is faster than the recrystallization of BDP in the aqueous solution, as discussed in the next section. This leads to a temporally supersaturated solution. The relative rates of the dissolution, the release and the recrystallization of BDP determine the maximum drug concentration and the timeframe of the solubilization effect, i.e. the release profile [58,59]. This kinetic phenomenon is termed as the spring effect in the literature. A mathematical model was developed by Hirai et.al. to describe the release profiles in the case of fast, but diffusion-limited drug release and slower recrystallization, as summarized in eq. (3) in Section 2.7 [31]. This model adequately describes the drug release profiles measured in the present study by using a single data set for the kinetic and solubility parameters, and varying the starting amount of the BDP-loaded aerogel carrier (Fig. 6b). The details on the kinetic modeling are given in the Supporting Information. The successful modeling further corroborates the above proposed mechanistic considerations for the explanation of the enhanced solubilization.

In order to gain further insights into the drug release mechanism, the hydration and wetting of the alginate aerogel carrier was studied in detail. Unfortunately, the fast hydration process of the aerogel could not be followed in real time, thus, a direct comparison with the release profiles is not possible. Nevertheless, the hydration process was elucidated based on the structures of multiple gradually hydrated aerogel samples characterized in their equilibrium states. The hydration mechanism reconstructed from these data can be related to the drug release profiles as follows.

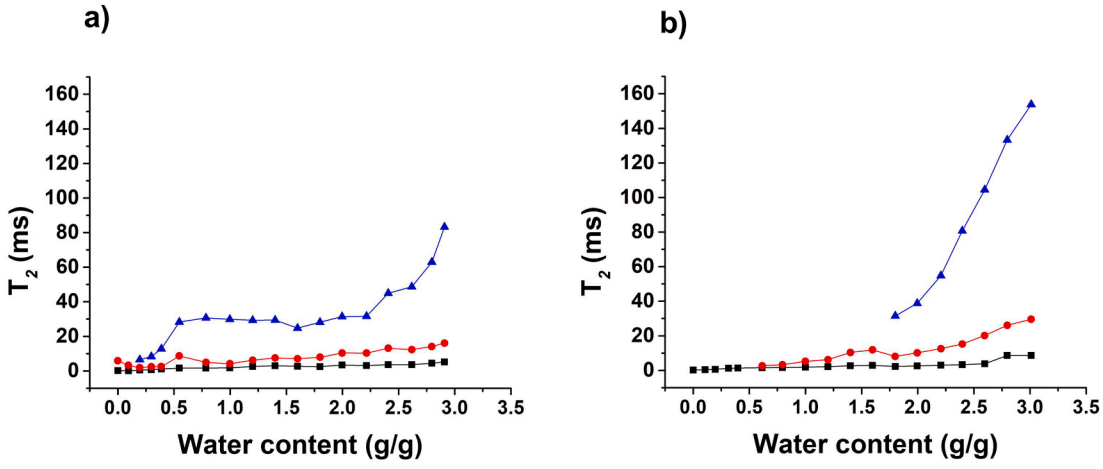

Fig. 7. NMR relaxometry of partially hydrated (a) pristine and (b) BDP-loaded alginate aerogels (first domain: black square, second domain: red circle, third domain: blue triangle). The deduced hydration mechanism is explained in the main text. Water content is given as grams of water per grams of dry aerogel. (For interpretation of the references to color in this figure legend, the reader is referred to the web version of this article.)

3.6. Hydration properties of pristine and BDP-loaded alginate aerogels

The hydration properties of pristine and BDP-loaded alginate aerogels were evaluated via NMR relaxometry as a means of predicting and understanding the behavior of the inhaled particles in aqueous respiratory fluid. The NMR relaxometry of water protons in hydrated solid backbones are based on the principle that the localization and chemical environment largely affect the ^{1}H relaxation times [32,61]. The water molecules in droplets and puddles do not interact directly with the solid alginate backbone and relax significantly slower than those that have strong bonds with the alginate network, such as in the primary hydration sphere [32,61]. A number of relaxation domains can be determined based on how quickly water molecules exchange between the different structural regions [32,61].

The measured T_2 (spin–spin) relaxation times in the pristine and the loaded aerogels are shown in Fig. 7 as a function of the water content of the samples. The series of the lowest T_2 values (first relaxation domain) represents strongly bound water inside the Ca-alginate fibers [30]. The evolution of the primary hydration sphere (second relaxation domain) that represents bound water on the top of the fibers, as well as the amount of quasi-bulk water in droplets and puddles (third relaxation domain), give information on the hydration and the wetting of the alginate aerogels [32,61]. It is noteworthy to compare the hydration profile of the present pristine alginate aerogel with another alginate aerogel described in the literature [30]. There are major differences in the hydration, namely the third domain representing water droplets appear at a much lower hydration level in the present alginate aerogel. This indicates that water easily forms a hydration layer and small droplets on the alginate fibers instead of penetrating into the fibers. Thus, the backbone of the present particular alginate aerogel is less prone to (partial) dissolution, swelling and hydrogel formation. All of these properties are beneficial for drug release, because the rate of repulsing the lipophilic drug from the surface can be higher, and the chance of trapping the drug in a hydrogel during release is lower.

The explanation for the special hydration properties of the present alginate aerogel is attributed to the single step exchange of water to absolute ethanol, whereas the reference material in the literature was prepared by multi-step gradual exchange of water to ethanol, as detailed in Table S1 in the Supporting Information [30]. The difference in the hydration profiles, as well as in the morphological parameters of the as-prepared aerogels are due to the molecular level and the nanoscale changes of the gel structures during the different solvent exchange procedures. Such phenomena are discussed in a recent paper [62]. The one-step solvent exchange process could have increased the resistance of the resulting alginate gel against dissolution by water, which is beneficial for the fast release of the loaded drug from the surface of the pores.

Comparing the hydration profiles of the pristine and the loaded alginate aerogels, the second domain (red circle) representing the primary hydration sphere appeared at a significantly later stage of hydration in the BDP-loaded aerogel. This is also true for the third domain of the water droplets, suggesting that the porous structure of the BDP-loaded aerogel was preserved better during hydration than that of the unloaded. In general, both of the second and third domains of the BDP-loaded alginate aerogels appeared later than in the pristine aerogel, which is due to the presence of BDP and the drug covering the pore walls of the alginate aerogels after SCF impregnation. Hence, the BDP-loaded alginate aerogels are more resistant to hydration-induced swelling and dissolution (degradation) compared to the unloaded alginate aerogels. Therefore, when the loaded aerogel contacts with water, BDP is expected to be repulsed by water before the aerogel structure collapses, which is well-aligned with the presence of the sudden burst in the first phase of the drug release profile.

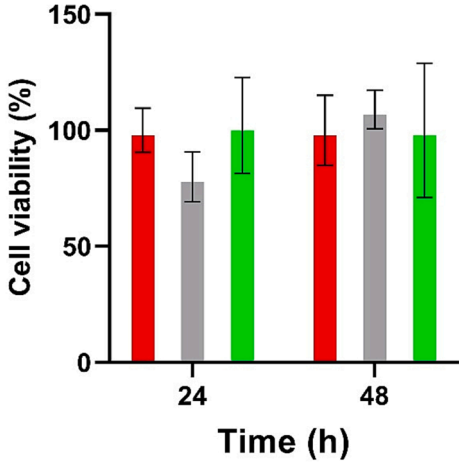

Fig. 8. Cell viability (%) after 24 and 48 h of incubation with calcium alginate aerogels and BDP-loaded alginate aerogels in relation to the non-treated cells as the negative control group (n = 3). Bar colour codes: Bars with red, grey and green color are used for negative control, alginate aerogel treatment and BDP-loaded alginate aerogel treatment, respectively. (For interpretation of the references to color in this figure legend, the reader is referred to the web version of this article.)

3.7. In vitro cytotoxicity tests

To assess the safety and potential of newly formulated substances, it is necessary to conduct *in vitro* cytotoxicity tests [33,34]. This study specifically examined the cytotoxicity of alginate aerogels crosslinked with calcium, as well as calcium alginate aerogels loaded with BDP using the NIH-3 T3 cell line for 24 and 48 h of incubation. The evaluation employed the resazurin method to measure cell viability, comparing the results to a negative control group that did not undergo treatment with alginate aerogels or the inhaled formulation.

As shown in Fig. 8, cell viability from alginate aerogels was not significantly lower than the negative control after 24 h (*ca.* 80 %), and similar to the negative control after 48 h. However, as defined in ISO 10993 standards, biomaterials are classified as cytotoxic if their impact results in less than 70 % cell viability [63]. Therefore, Ca-alginate aerogels demonstrated cytocompatibility. The inhaled formulation containing BDP-loaded alginate aerogels exhibited similar cell viability (%) after 24 and 48 h, indicating no cytotoxicity as well. Other *in vitro* studies demonstrated the high biocompatibility of Ca-alginate aerogels [64,65] and of BDP [33]. Hence, the obtained results confirmed that the inhaled formulation does not induce any cytotoxic effects.

3.8. Ex vivo bronchial permeability tests

In the treatment of asthma, it is very important to ensure that inhaled drugs are deposited predominantly in the bronchial tissue where inflammation and bronchoconstriction occur. The local drug deposition facilitates localized relief and effective treatment of asthma symptoms while minimizing the occurrence of systemic side effects [66]. In the present study, the capacity of the BDP released from the aerogels to permeate through and remain in the bronchial tissue was evaluated using porcine lungs. Porcine lungs are frequently employed in medical research studies to understand various respiratory diseases like cystic fibrosis and asthma, owing to their shared anatomical features and tissue compatibility with the human lungs [67,68].

The preparation of Franz cells for the *ex vivo* permeability study is illustrated in Fig. 9a. Both pure BDP and BDP released from the aerogel particles were able to similarly permeate through the bronchial tissue during the first hour of the experiment with no statistically significant differences between them (Fig. 9b). There was also no statistically significant differences between the permeated drug from pure BDP when summarizing the two hours. However, the permeated drug amount after 2 h was higher in the case of pure BDP when compared to the aerogel formulations. These differences in permeation after 2 h were related to

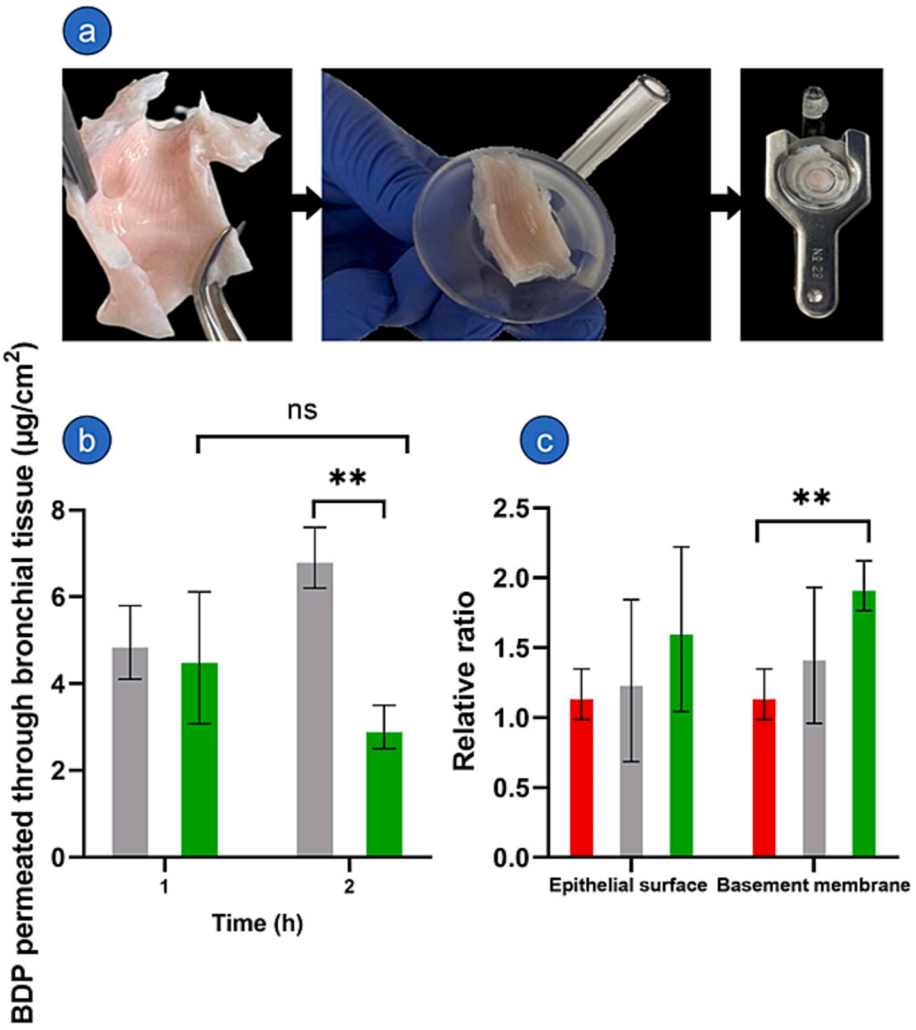

Fig. 9. *Ex vivo* permeability tests: (a) Preparation of Franz cells for the study; (b) cumulative amounts of BDP permeated through porcine bronchial tissue (n = 3; mean values and standard deviations); (c) relative intensity ratio of Raman peaks indicating the presence of BDP in the epithelial surface and in the tissue basement membrane layer. Bar code: Bars with red, grey and green color were used for blank tissue, BDP powder and BDP-loaded alginate aerogels, respectively. (For interpretation of the references to color in this figure legend, the reader is referred to the web version of this article.)

the formulation properties as well as to other limitations of the experimental approach. Although the pure BDP and the aerogel formulation used in this test contained an equivalent amount of BDP, the aerogel formulation had a higher total weight and occupied a much higher volume compared to pure BDP due to the presence of alginate as drug carrier. The lower weights used in pure BDP formulations resulted in a direct contact of the drug with the porcine epithelium surface in the Franz cell and in a subsequent high amount of BDP permeated after 2 h. In contrast, the higher quantity and volume of the aerogel formulation compared to BDP powder, led to higher sample thicknesses on the surface of the tissue hampering the direct contact of the aerogel with the epithelial tissue and, subsequently, reducing the drug release and permeation. This situation observed with the aerogels is shared with commercial inhaled formulations, as they have high weight proportions of lactose as excipients in their formulations. It should be also noted that the actual permeated drug should be higher in a real biological environment as the available permeation area in the Franz cells (0.785 cm^2) of this study was significantly lower than the actual epithelial surface area in the human body. Experiments with aerogels had high standard deviations mainly due to the complex procedure of adding reproducible and homogeneous alginate gel thicknesses on the surface of the epithelial tissues for all the replicates, as particles tended to form clusters or adhere to the walls of Franz cells in the donor chamber. Finally, the HPLC method was not able to quantify the permeated BDP after 3 h in none of the formulations, likely due to the dilution effect caused by replacing the liquid aliquots with fresh medium at different times.

IR-Raman spectroscopy analysis was conducted following the permeation experiments to confirm the presence of BDP in the bronchial tissue (Fig. 9c). The evaluation consisted of comparing the Raman peaks between blank tissue (no BDP treatment), and pure BDP or BDP-loaded aerogel treated tissues in the epithelial surface (in contact with the donor chamber) and the basement membrane (in contact with the receptor chamber) sections of the tissue. The analysis was conducted using a relative quantification to a reference Raman peak measured in fresh untreated tissue pieces (cf. Section 2.10.2). In the surface tissue section of samples treated with the BDP-loaded aerogel particles, a higher amount of incorporated BDP was measured than in the samples treated with pure BDP, although not statistically different. However, in the basement membrane layer of the bronchial tissue, the presence of BDP was detected with statistical significance confirming the permeation of the drug through the bronchial tissue. Furthermore, the tissue samples treated with the BDP-loaded alginate aerogels had higher amounts of the drug with statistically significant differences compared with the blank tissue.

Overall, the results showed positive aspects of the aerogel formulation for pulmonary BDP delivery suggesting that these specifically

designed aerogel particles can effectively achieve a local drug deposition within the bronchial tissue.

4. Conclusions

It has been demonstrated that nanostructured calcium alginate aerogel microspheres prepared by compressed air-assisted prilling gelation and drying in $scCO_2$ are effective drug delivery vehicles for novel inhaled formulations. The alginate aerogel microparticles have high flowability, low inter-particular stacking, and optimal aerodynamic sizes of 1–5 μm predicting deep lung penetration. Furthermore, the co-solvent assisted $scCO_2$ impregnation preserves the porous nanostructure of alginate aerogels and provides high BDP loading efficiency, as well as yields the amorphous form of the drug. The presented novel formulation has a higher drug-to-excipient ratio than representative commercial formulations, giving it the advantage of high doses. The *in vitro* drug release pattern starts with a burst, which is explained by the fast and facile hydration of the alginate carrier that repels the drug molecules from the pores. The examination of the hydration mechanism of the formulations also reveals that the alginate aerogels loaded with BDP preserves their nanostructure more effectively compared to the pristine alginate aerogels during partial hydration. This is advantageous for the fast release and the effective solubilization of the drug. The *in vitro* cytotoxicity tests confirm no harmful effects from the inhaled formulation based on alginate aerogels. The *ex vivo* bronchial permeability tests indicate that BDP released from the aerogel carrier is effectively localized within the porcine bronchial tissues, even when compared to using pure BDP without excipient.

CRediT authorship contribution statement

Thoa Duong: Writing – review & editing, Writing – original draft, Methodology, Investigation. **Maria Vivero-Lopez:** Writing – review & editing, Methodology, Investigation. **Inés Ardao:** Investigation, Methodology, Writing – review & editing. **Carmen Alvarez-Lorenzo:** Writing – review & editing, Supervision, Methodology. **Attila Forgács:** Writing – review & editing, Methodology, Investigation. **József Kalmár:** Writing – review & editing, Writing – original draft, Supervision, Methodology, Investigation, Funding acquisition, Conceptualization. **Carlos A. García-González:** Writing – review & editing, Writing – original draft, Supervision, Methodology, Investigation, Funding acquisition, Conceptualization.

Declaration of competing interest

The authors declare that they have no known competing financial interests or personal relationships that could have appeared to influence the work reported in this paper.

Data availability

Data will be made available on request.

Acknowledgments

Work supported by MICINN [PID2020-120010RB-I00/AEI/10.13039/501100011033], Xunta de Galicia [ED431C 2020/17], Agencia Estatal de Investigación [AEI] and FEDER funds. This publication is based on work from AERoGELS COST Action (ref. CA18125) supported by COST (European Cooperation in Science and Technology). Th. D. acknowledges the support of Diputación Provincial de A Coruña for research in health science 2022-2023 (BINV-CS/2022) and of AERoGELS COST Action (ref. CA18125) for a Short Term Scientific Missions (STSM) grant, enabling for the collaboration with HUN-REN-DE Mechanisms of Complex Homogeneous and Heterogeneous Chemical Reactions Research Group, Department of Inorganic and Analytical Chemistry, University of Debrecen (Hungary). The authors would like to thank Ezequiel Vázquez Fernández (University of Santiago de Compostela, Spain), Laura Juhász and Krisztián Moldován (University of Debrecen, Hungary) for their valuable support and technical help with Raman spectroscopy, X-ray diffraction, IR-ATR and SEM analyses.

Appendix A. Supplementary data

Supplementary data to this article can be found online at https://doi.org/10.1016/j.cej.2024.149849.

References

[1] B. Chaurasiya, Y.-Y. Zhao, Dry powder for pulmonary delivery: a comprehensive review, Pharmaceutics 13 (2020) 31, https://doi.org/10.3390/pharmaceutics13010031.
[2] A.J. Plaunt, T.L. Nguyen, M.R. Corboz, V.S. Malinin, D.C. Cipolla, Strategies to overcome biological barriers associated with pulmonary drug delivery, Pharmaceutics 14 (2022) 302, https://doi.org/10.3390/pharmaceutics14020302.
[3] R. Li, Y. Jia, X. Kong, Y. Nie, Y. Deng, Y. Liu, Novel drug delivery systems and disease models for pulmonary fibrosis, J. Controlled Release 348 (2022) 95–114, https://doi.org/10.1016/j.jconrel.2022.05.039.
[4] C. Moon, H.D.C. Smyth, A.B. Watts, R.O. Williams, Delivery technologies for orally inhaled products: an update, AAPS PharmSciTech 20 (2019) 117, https://doi.org/10.1208/s12249-019-1314-2.
[5] C. Gregoriano, T. Dieterle, A.-L. Breitenstein, S. Dürr, A. Baum, S. Maier, I. Arnet, K.E. Hersberger, J.D. Leuppi, Use and inhalation technique of inhaled medication in patients with asthma and COPD: data from a randomized controlled trial, Respir. Res. 19 (2018) 237, https://doi.org/10.1186/s12931-018-0936-3.
[6] S.S. Kunde, R. Ghosh, S. Wairkar, Emerging trends in pulmonary delivery of biopharmaceuticals, Drug Discov. Today 27 (2022) 1474–1482, https://doi.org/10.1016/j.drudis.2022.02.003.
[7] T. Duong, C. López-Iglesias, P.K. Szewczyk, U. Stachewicz, J. Barros, C. Alvarez-Lorenzo, M. Alnaief, C.A. García-González, A pathway from porous particle technology toward tailoring aerogels for pulmonary drug administration, Front. Bioeng. Biotechnol. 9 (2021) 671381, https://doi.org/10.3389/fbioe.2021.671381.
[8] C.A. García-González, T. Budtova, L. Durães, C. Erkey, P. Del Gaudio, P. Gurikov, M. Koebel, F. Liebner, M. Neagu, I. Smirnova, An opinion paper on aerogels for biomedical and environmental applications, Molecules 24 (2019) 1815, https://doi.org/10.3390/molecules24091815.
[9] C. López-Iglesias, A.M. Casielles, A. Altay, R. Bettini, C. Alvarez-Lorenzo, C. A. García-González, From the printer to the lungs: Inkjet-printed aerogel particles for pulmonary delivery, Chem. Eng. J. 357 (2019) 559–566, https://doi.org/10.1016/j.cej.2018.09.159.
[10] M. Alnaief, R.M. Obaidat, M.M. Alsmadi, Preparation of hybrid alginate-chitosan aerogel as potential carriers for pulmonary drug delivery, Polymers 12 (2020) 2223, https://doi.org/10.3390/polym12102223.
[11] C.A. García-González, A. Sosnik, J. Kalmár, I. De Marco, C. Erkey, A. Concheiro, C. Alvarez-Lorenzo, Aerogels in drug delivery: From design to application, J. Controlled Release 332 (2021) 40–63, https://doi.org/10.1016/j.jconrel.2021.02.012.
[12] T. Athamneh, A. Amin, E. Benke, R. Ambrus, C.S. Leopold, P. Gurikov, I. Smirnova, Alginate and hybrid alginate-hyaluronic acid aerogel microspheres as potential carrier for pulmonary drug delivery, J. Supercrit. Fluids 150 (2019) 49–55, https://doi.org/10.1016/j.supflu.2019.04.013.
[13] B.P. Vinjamuri, A.K. Kotha, A. Kolte, R.V. Haware, M.B. Chougule, Polymer Applications in Pulmonary Drug Delivery, in: Appl. Polym. Drug Deliv., Elsevier, 2021: pp. 333–354. https://doi.org/10.1016/B978-0-12-819659-5.00012-4.
[14] M.F. Aldawsari, M.M. Ahmed, F. Fatima, M.K. Anwer, P. Katakam, A. Khan, Development and characterization of calcium-alginate beads of apigenin. in vitro antitumor, antibacterial, and antioxidant activities, Mar. Drugs 19 (2021) 467, https://doi.org/10.3390/md19080467.
[15] T. Athamneh, A. Amin, E. Benke, R. Ambrus, P. Gurikov, I. Smirnova, C.S. Leopold, Pulmonary drug delivery with aerogels: engineering of alginate and alginate–hyaluronic acid microspheres, Pharm. Dev. Technol. 26 (2021) 509–521, https://doi.org/10.1080/10837450.2021.1888979.
[16] S. van Koningsbruggen-Rietschel, J.C. Davies, T. Pressler, R. Fischer, G. MacGregor, S.H. Donaldson, K. Smerud, N. Meland, J. Mortensen, M.Ø. Fosbøl, D.G. Downey, A.H. Myrset, H. Flaten, P.D. Rye, Inhaled dry powder alginate oligosaccharide in cystic fibrosis: a randomised, double-blind, placebo-controlled, crossover phase 2b study, ERJ Open Res. 6 (2020) 00132–02020, https://doi.org/10.1183/23120541.00132-2020.
[17] J.F.A. Valente, J.R. Dias, A. Sousa, N. Alves, Composite central face design—an approach to achieve efficient alginate microcarriers, Polymers 11 (2019) 1949, https://doi.org/10.3390/polym11121949.
[18] K. Ganesan, T. Budtova, L. Ratke, P. Gurikov, V. Baudron, I. Preibisch, P. Niemeyer, I. Smirnova, B. Milow, Review on the production of polysaccharide aerogel particles, Materials 11 (2018) 2144, https://doi.org/10.3390/ma11112144.
[19] C.A. García-González, M.C. Camino-Rey, M. Alnaief, C. Zetzl, I. Smirnova, Supercritical drying of aerogels using CO_2: Effect of extraction time on the end

material textural properties, J. Supercrit. Fluids 66 (2012) 297–306, https://doi.org/10.1016/j.supflu.2012.02.026.
[20] İ. Şahin, Y. Özbakır, Z. İnönü, Z. Ulker, C. Erkey, Kinetics of supercritical drying of gels, Gels 4 (2017) 3, https://doi.org/10.3390/gels4010003.
[21] D. Hidayat, W. Widiyastuti, T. Ogi, K. Okuyama, Droplet generation and nanoparticle formation in low-pressure spray pyrolysis, Aerosol Sci. Technol. 44 (2010) 692–705, https://doi.org/10.1080/02786826.2010.486684.
[22] K.A. Kravanja, M. Finšgar, Ž. Knez, M. Knez Marevci, Supercritical fluid technologies for the incorporation of synthetic and natural active compounds into materials for drug formulation and delivery, Pharmaceutics 14 (2022) 1670, https://doi.org/10.3390/pharmaceutics14081670.
[23] J.L. Gómez-Amoza, Tratado de tecnología farmacéutica, Ramón Martínez Pacheco, Editorial Síntesis S.A, Madrid, Spain, 2016.
[24] P. Gurikov, I. Smirnova, Amorphization of drugs by adsorptive precipitation from supercritical solutions: A review, J. Supercrit. Fluids 132 (2018) 105–125, https://doi.org/10.1016/j.supflu.2017.03.005.
[25] L. Juhász, K. Moldován, P. Gurikov, F. Liebner, I. Fábián, J. Kalmár, C. Cserháti, False morphology of aerogels caused by gold coating for SEM imaging, Polymers 13 (2021) 588, https://doi.org/10.3390/polym13040588.
[26] R.W. Dal Negro, Dry powder inhalers and the right things to remember: a concept review, Multidiscip. Respir. Med. 10 (2015) 13, https://doi.org/10.1186/s40248-015-0012-5.
[27] C. Jaafar-Maalej, V. Andrieu, A. Elaissari, H. Fessi, Beclomethasone-loaded lipidic nanocarriers for pulmonary drug delivery: preparation, characterization and in vitro drug release, J. Nanosci. Nanotechnol. 11 (2011) 1841–1851, https://doi.org/10.1166/jnn.2011.3119.
[28] I. Khan, S. Yousaf, M. Najlah, W. Ahmed, A. Elhissi, Proliposome powder or tablets for generating inhalable liposomes using a medical nebulizer, J. Pharm. Investig. 51 (2021) 61–73, https://doi.org/10.1007/s40005-020-00495-8.
[29] P. Veres, M. Kéri, I. Bányai, I. Lázár, I. Fábián, C. Domingo, J. Kalmár, Mechanism of drug release from silica-gelatin aerogel—Relationship between matrix structure and release kinetics, Colloids Surf. B Biointerfaces 152 (2017) 229–237, https://doi.org/10.1016/j.colsurfb.2017.01.019.
[30] M. Kéri, A. Forgács, V. Papp, I. Bányai, P. Veres, A. Len, Z. Dudás, I. Fábián, J. Kalmár, Gelatin content governs hydration induced structural changes in silica-gelatin hybrid aerogels – Implications in drug delivery, Acta Biomater. 105 (2020) 131–145, https://doi.org/10.1016/j.actbio.2020.01.016.
[31] D. Hirai, Y. Iwao, S.-I. Kimura, S. Noguchi, S. Itai, Mathematical model to analyze the dissolution behavior of metastable crystals or amorphous drug accompanied with a solid-liquid interface reaction, Int. J. Pharm. 522 (2017) 58–65, https://doi.org/10.1016/j.ijpharm.2017.02.050.
[32] A. Forgács, V. Papp, G. Paul, L. Marchese, A. Len, Z. Dudás, I. Fábián, P. Gurikov, J. Kalmár, Mechanism of hydration and hydration induced structural changes of calcium alginate aerogel, ACS Appl. Mater. Interfaces 13 (2021) 2997–3010, https://doi.org/10.1021/acsami.0c17012.
[33] J.M. Chassot, D. Ribas, E.F. Silveira, L.D. Grünspan, C.C. Pires, P.V. Farago, E. Braganhol, L. Tasso, L. Cruz, Beclomethasone dipropionate-loaded polymeric nanocapsules: development, in vitro cytotoxicity, and in vivo evaluation of acute lung injury, J. Nanosci. Nanotechnol. 15 (2015) 855–864, https://doi.org/10.1166/jnn.2015.9178.
[34] A.M. Rahimi, M. Cai, S. Hoyer-Fender, Heterogeneity of the NIH3T3 Fibroblast Cell Line, Cells 11 (2022) 2677, https://doi.org/10.3390/cells11172677.
[35] E.M. Longhin, N. El Yamani, E. Rundén-Pran, M. Dusinska, The alamar blue assay in the context of safety testing of nanomaterials, Front. Toxicol. 4 (2022) 981701, https://doi.org/10.3389/ftox.2022.981701.
[36] A. Veronovski, Ž. Knez, Z. Novak, Preparation of multi-membrane alginate aerogels used for drug delivery, J. Supercrit. Fluids 79 (2013) 209–215, https://doi.org/10.1016/j.supflu.2013.01.025.
[37] A. Vatanara, A. Najafabadi, M. Khajeh, Y. Yamini, Solubility of some inhaled glucocorticoids in supercritical carbon dioxide, J. Supercrit. Fluids 33 (2005) 21–25, https://doi.org/10.1016/S0896-8446(04)00112-3.
[38] G. Caputo, M. Scognamiglio, I. De Marco, Nimesulide adsorbed on silica aerogel using supercritical carbon dioxide, Chem. Eng. Res. Des. 90 (2012) 1082–1089, https://doi.org/10.1016/j.cherd.2011.11.011.
[39] P. Chakravarty, A. Famili, K. Nagapudi, M.A. Al-Sayah, Using supercritical fluid technology as a green alternative during the preparation of drug delivery systems, Pharmaceutics 11 (2019) 629, https://doi.org/10.3390/pharmaceutics11120629.
[40] Fostair NEXThaler 200 micrograms/6 micrograms per actuation inhalation powder - Summary of Product Characteristics (SmPC) - (emc), (n.d.). https://www.medicines.org.uk/emc/product/5075/smpc#gref (accessed January 25, 2023).
[41] Seebri Breezhaler 44 micrograms inhalation powder, hard capsules - Summary of Product Characteristics (SmPC) - (emc), (n.d.). https://www.medicines.org.uk/emc/product/2840/smpc#gref (accessed January 25, 2023).
[42] A.H. de Boer, P. Hagedoorn, M. Hoppentocht, F. Buttini, F. Grasmeijer, H. W. Frijlink, Dry powder inhalation: past, present and future, Expert Opin. Drug Deliv. 14 (2017) 499–512, https://doi.org/10.1080/17425247.2016.1224846.
[43] J. Weers, A. Clark, The impact of inspiratory flow rate on drug delivery to the lungs with dry powder inhalers, Pharm. Res. 34 (2017) 507–528, https://doi.org/10.1007/s11095-016-2050-x.
[44] L. Casula, F. Lai, E. Pini, D. Valenti, C. Sinico, M.C. Cardia, S. Marceddu, G. Ailuno, A.M. Fadda, Pulmonary delivery of curcumin and beclomethasone dipropionate in a multicomponent nanosuspension for the treatment of bronchial asthma, Pharmaceutics 13 (2021) 1300, https://doi.org/10.3390/pharmaceutics13081300.
[45] M. PantiĽ, P. Kotnik, Ž. Knez, Z. Novak, High pressure impregnation of vitamin D3 into polysaccharide aerogels using moderate and low temperatures, J. Supercrit. Fluids 118 (2016) 171–177, https://doi.org/10.1016/j.supflu.2016.08.008.
[46] D. Yang, Q. Jiang, J. Ma, B. Guo, Y. Li, P. Ma, T. Zhang, Nisoldipine dissolution profile enhancement by supercritical carbon dioxide impregnation technique with fumed silica, Powder Technol. 271 (2015) 7–15, https://doi.org/10.1016/j.powtec.2014.11.014.
[47] L. Wijayanti, S. Setiasih, S. Hudiyono, Encapsulation of bromelain in alginate-carboxymethyl cellulose microspheres as an antiplatelet agent, J. Phys. Conf. Ser. 1943 (2021) 012165, https://doi.org/10.1088/1742-6596/1943/1/012165.
[48] G. Helmiyati, G.H. Novientri, E. Abbas, Budianto, Nanocomposite hydrogel-based biopolymer modified with silver nanoparticles as an antibacterial material for wound treatment, J. Appl. Pharm. Sci. 9 (2019) 1–9, https://doi.org/10.7324/JAPS.2019.91101.
[49] H.-T. Wu, Y.-H. Chuang, H.-C. Lin, T.-C. Hu, Y.-J. Tu, L.-J. Chien, Immediate release formulation of inhaled beclomethasone dipropionate-hydroxypropyl-beta-cyclodextrin composite particles produced using supercritical assisted atomization, Polymers 14 (2022) 2114, https://doi.org/10.3390/polym14102114.
[50] M. Champeau, J.-M. Thomassin, T. Tassaing, C. Jérôme, Drug loading of polymer implants by supercritical CO_2 assisted impregnation: A review, J. Controlled Release 209 (2015) 248–259, https://doi.org/10.1016/j.jconrel.2015.05.002.
[51] A. Torge, G. Pavone, M. Jurisic, K. Lima-Engelmann, M. Schneider, A comparison of spherical and cylindrical microparticles composed of nanoparticles for pulmonary application, Aerosol Sci. Technol. 53 (2019) 53–62, https://doi.org/10.1080/02786826.2018.1542484.
[52] A.M. Healy, M.I. Amaro, K.J. Paluch, L. Tajber, Dry powders for oral inhalation free of lactose carrier particles, Adv. Drug Deliv. Rev. 75 (2014) 32–52, https://doi.org/10.1016/j.addr.2014.04.005.
[53] A.J. Hickey, D.A. Edwards, Density and shape factor terms in stokes' equation for aerodynamic behavior of aerosols, J. Pharm. Sci. 107 (2018) 794–796, https://doi.org/10.1016/j.xphs.2017.11.005.
[54] B.B. Eedara, R. Bastola, S.C. Das, Dissolution and absorption of inhaled drug particles in the lungs, Pharmaceutics 14 (2022) 2667, https://doi.org/10.3390/pharmaceutics14122667.
[55] I. van der Zwaan, F. Franek, R. Fransson, U. Tehler, G. Frenning, Characterization of membrane-type dissolution profiles of clinically available orally inhaled products using a weibull fit and a mechanistic model, Mol. Pharm. 19 (2022) 3114–3124, https://doi.org/10.1021/acs.molpharmaceut.2c00177.
[56] T. Riley, D. Christopher, J. Arp, A. Casazza, A. Colombani, A. Cooper, M. Dey, J. Maas, J. Mitchell, M. Reiners, N. Sigari, T. Tougas, S. Lyapustina, Challenges with developing in vitro dissolution tests for orally inhaled products (OIPs), AAPS PharmSciTech 13 (2012) 978–989, https://doi.org/10.1208/s12249-012-9822-3.
[57] J.E. Hastedt, P. Bäckman, A.R. Clark, W. Doub, A. Hickey, G. Hochhaus, P.J. Kuehl, C.-M. Lehr, P. Mauser, J. McConville, R. Niven, M. Sakagimi, J.G. Weers, Scope and relevance of a pulmonary biopharmaceutical classification system AAPS/FDA/USP Workshop March 16–17th, 2015 in Baltimore, MD, AAPS Open 2 (2016) 1, https://doi.org/10.1186/s41120-015-0002-x.
[58] PubChem, Beclomethasone dipropionate, (n.d.). https://pubchem.ncbi.nlm.nih.gov/compound/21700 (accessed October 5, 2023).
[59] C. Potter, Y. Tian, G. Walker, C. McCoy, P. Hornsby, C. Donnelly, D.S. Jones, G. P. Andrews, Novel supercritical carbon dioxide impregnation technique for the production of amorphous solid drug dispersions: a comparison to hot melt extrusion, Mol. Pharm. 12 (2015) 1377–1390, https://doi.org/10.1021/mp500644h.
[60] D.E. Alonzo, Y. Gao, D. Zhou, H. Mo, G.G.Z. Zhang, L.S. Taylor, Dissolution and precipitation behavior of amorphous solid dispersions, J. Pharm. Sci. 100 (2011) 3316–3331, https://doi.org/10.1002/jps.22579.
[61] I. Lázár, A. Forgács, A. Horváth, G. Király, G. Nagy, A. Len, Z. Dudás, V. Papp, Z. Balogh, K. Moldován, L. Juhász, C. Cserháti, Z. Szántó, I. Fábián, J. Kalmár, Mechanism of hydration of biocompatible silica-casein aerogels probed by NMR and SANS reveal backbone rigidity, Appl. Surf. Sci. 531 (2020) 147232, https://doi.org/10.1016/j.apsusc.2020.147232.
[62] A. Hajnal, M.L. Aiyelari, M. Dirauf, P. Gurikov, Investigation of the uniformity of gel shrinkage by imaging tracer particles using X-Ray microtomography, Adv. Eng. Mater. (2023) 2301423, https://doi.org/10.1002/adem.202301423.
[63] E. Jablonská, J. Kubásek, D. Vojtěch, T. Ruml, J. Lipov, Test conditions can significantly affect the results of in vitro cytotoxicity testing of degradable metallic biomaterials, Sci. Rep. 11 (2021) 6628, https://doi.org/10.1038/s41598-021-85019-6.
[64] M.A.A. Al-Najjar, T. Athamneh, R. AbuTayeh, I. Basheti, C. Leopold, P. Gurikov, I. Smirnova, Evaluation of the orally administered calcium alginate aerogel on the changes of gut microbiota and hepatic and renal function of Wistar rats, PLOS ONE 16 (2021) e0247633, https://doi.org/10.1371/journal.pone.0247633.
[65] P. Franco, E. Pessolano, R. Belvedere, A. Petrella, I. De Marco, Supercritical impregnation of mesoglycan into calcium alginate aerogel for wound healing,

J. Supercrit. Fluids 157 (2020) 104711, https://doi.org/10.1016/j.supflu.2019.104711.
[66] J. Shao, Y. Wang, G. Hochhaus, Semi-mechanistic PK/PD model to assess pulmonary targeting of beclomethasone dipropionate and its active metabolite, Eur. J. Pharm. Sci. 159 (2021) 105699, https://doi.org/10.1016/j.ejps.2021.105699.
[67] N. Bertho, F. Meurens, The pig as a medical model for acquired respiratory diseases and dysfunctions: An immunological perspective, Mol. Immunol. 135 (2021) 254–267, https://doi.org/10.1016/j.molimm.2021.03.014.
[68] E.P. Judge, J.M.L. Hughes, J.J. Egan, M. Maguire, E.L. Molloy, S. O'Dea, Anatomy and bronchoscopy of the porcine lung. a model for translational respiratory medicine, Am. J. Respir. Cell Mol. Biol. 51 (2014) 334–343, https://doi.org/10.1165/rcmb.2013-0453TR.